JBC RESEARCH ARTICLE

Disruption of *Ephx2* in cardiomyocytes but not endothelial cells improves functional recovery after ischemia-reperfusion in isolated mouse hearts

Received for publication, February 17, 2022, and in revised form, February 10, 2023 Published, Papers in Press, February 22, 2023,
https://doi.org/10.1016/j.jbc.2023.103049

Matthew L. Edin[1], Artiom Gruzdev[1], J. Alyce Bradbury[1], Joan P. Graves[1], Fred B. Lih[1], Laura M. DeGraff[1], Ingrid Fleming[2], and Darryl C. Zeldin[1,*]

From the [1]Division of Intramural Research, National Institute for Environmental Health Sciences, National Institutes of Health, Research Triangle Park, North Carolina, USA; [2]Institute for Vascular Signaling, Centre of Molecular Medicine, Goethe University, Frankfurt am Main, Germany

Reviewed by members of the JBC Editorial Board. Edited by George M. Carman

Cytochromes P450 metabolize arachidonic acid to epoxyeicosatrienoic acids (EETs) which have numerous effects. After cardiac ischemia, EET-induced coronary vasodilation increases delivery of oxygen/nutrients to the myocardium, and EET-induced signaling protects cardiomyocytes against post-ischemic mitochondrial damage. Soluble epoxide hydrolase 2 (EPHX2) diminishes the benefits of EETs through hydrolysis to less active dihydroxyeicosatrienoic acids. EPHX2 inhibition or genetic disruption improves recovery of cardiac function after ischemia. Immunohistochemical staining revealed EPHX2 expression in cardiomyocytes and some endothelial cells but little expression in cardiac smooth muscle cells or fibroblasts. To determine specific roles of EPHX2 in cardiac cell types, we generated mice with cell-specific disruption of *Ephx2* in endothelial cells (*Ephx2*$^{fx/fx}$*/Tek-cre*) or cardiomyocytes (*Ephx2*$^{fx/fx}$*/Myh6-cre*) to compare to global *Ephx2*-deficient mice (global *Ephx2*$^{-/-}$) and WT (*Ephx2*$^{fx/fx}$) mice in expression, EET hydrolase activity, and heart function studies. Most cardiac EPHX2 expression and activity is in cardiomyocytes with substantially less activity in endothelial cells. *Ephx2*$^{fx/fx}$*/Tek-cre* hearts have similar EPHX2 expression, hydrolase activity, and postischemic cardiac function as control *Ephx2*$^{fx/fx}$ hearts. However, *Ephx2*$^{fx/fx}$*/Myh6-cre* hearts were similar to global *Ephx2*$^{-/-}$ hearts with significantly diminished EPHX2 expression, decreased hydrolase activity, and enhanced postischemic cardiac function compared to *Ephx2*$^{fx/fx}$ hearts. During reperfusion, *Ephx2*$^{fx/fx}$*/Myh6-cre* hearts displayed increased ERK activation compared to *Ephx2*$^{fx/fx}$ hearts, which could be reversed by EEZE treatment. EPHX2 did not regulate coronary vasodilation in this model. We conclude that EPHX2 is primarily expressed in cardiomyocytes where it regulates EET hydrolysis and postischemic cardiac function, whereas endothelial EPHX2 does not play a significant role in these processes.

Cytochromes P450 can oxidize arachidonic acid to form epoxyeicosatrienoic acids (EETs) that have potent biological effects, including vasodilatory, angiogenic, anti-inflammatory, cytoprotective, and antinociceptive properties (1). These P450s can also generate other epoxy-fatty acids (EpFAs), such as epoxyoctadecamonoenoic acid (EpOMEs), epoxyeicosatetraenoic acids (EpETEs), and epoxydocosapentaenoic acids (EpDPEs) which are derived from linoleic acid (LA), eicosapentaenoic acid (EPA), or docosahexaenoic acid (DHA), respectively (2). The effects of these EpFAs are typically short-lived due to hydrolysis to biologically less-active diols by epoxide hydrolases (EPHXs). Together, both microsomal epoxide hydrolase (EPHX1/mEH) and soluble epoxide hydrolase (EPHX2) account for nearly all EpFA hydrolysis *in vivo* (3). Pharmacological inhibition of EPHX2 potentiates the effects of endogenous EETs and shows promise for the treatment of a variety of cardiovascular diseases in preclinical models (4).

While EET treatment or EPHX2 inhibition is protective against postischemic cardiac reperfusion injury (5, 6), numerous questions remain. For example, heart ventricles consist of approximately 50% cardiomyocytes, 20% pericytes and smooth muscle cells, 15% fibroblasts, 8% endothelial cells, and 5% immune cells (7, 8); however, few have investigated which of these cardiac cell types express EPHX2. EPHX2 has been detected in "human coronary artery and surrounding tissues" (9) as well as in "blood vessels and myocardium" (10). Vascular beds in other tissues suggest strong staining for EPHX2 in both endothelial and smooth muscle cells (11, 12). The extent to which various cell types contribute to overall cardiac EET hydrolysis has not been investigated. Importantly, it remains to be determined the extent to which cellular EPHX2 expression, and concomitant EET hydrolysis, regulate postischemic cardiovascular functions.

Potentiation of EpFA signaling in vascular cells may regulate multiple biological processes to limit myocardial infarction and/or improve postischemic cardiac functional recovery. Myocardial infarction occurs after atherosclerotic narrowing of coronary arteries due to plaque rupture and/or thrombus formation. Occlusion of coronary vessels prevents blood, oxygen, and nutrient flow to the myocardium which results in tissue injury or death. EPHX2 inhibition is anti-inflammatory and might lessen the likelihood of myocardial infarction by

* For correspondence: Darryl C. Zeldin, zeldin@niehs.nih.gov.

reducing atherosclerotic plaque formation or progression (13–15). During or after myocardial infarction, EPHX2 inhibition could also reduce infarction by increasing EETs, which have antithrombolytic effects (16). Expression of EPHX2 in either endothelial cells or smooth muscle could also regulate EET-induced vasodilation which could increase blood flow through narrowed or partially occluded coronary arteries to improve delivery of oxygen and nutrients and removal of waste products (17).

In addition to effects on blood or vascular cells, EETs protect cardiomyocytes during ischemia-reperfusion (I/R) injury. Several multiprotein complexes, including ATP-sensitive K^+ channels (K_{ATP}) and the mitochondrial permeability transition pore (mPTP), play key roles in mitochondrial responses after ischemia. In nonischemic conditions, the mPTP remains closed, which maintains mitochondrial membrane potential. mPTP opening in response to reperfusion-induced oxidative stress results in the leakage of large molecules, loss of membrane potential, uncoupling of oxidative phosphorylation, and ultimately leads to cell death (18). Hearts with elevated EETs have increased activation of PI3 kinase, AKT, and/or ERK during early reperfusion (6, 19). These signaling cascades can result in inhibitory GSK-3β phosphorylation that suppresses mPTP opening (20). EETs also bind and increase the opening of K_{ATP} channels (21). Although the mechanism is unclear, K_{ATP} channel activation by EETs significantly improves cardiac recovery from ischemia (6, 19).

Genetic ablation or inhibition of EPHX2 has also revealed its role in other cardiovascular pathologies. *Ephx2*$^{-/-}$ mice are protected against lipopolysaccharide-induced cardiac inflammation and dysfunction (22), and EPHX2 regulates the development of cardiomyopathy and heart failure (23–25). Multiple studies implicate EPHX2 polymorphisms in the incidence or recurrence of myocardial infarction (26, 27). Interpretation of these studies is often vague or inadequate given the poor understanding of the cellular distribution of EPHX2 in the heart.

In this manuscript, we define the relative contribution of EPHX2 expression in distinct cellular compartments to EET hydrolysis and postischemic cardiac functional recovery. We generated mice with selective disruption of *Ephx2* in endothelial cells or cardiomyocytes and compared them to WT mice and mice with global *Ephx2* disruption. We characterized the relative contribution of endothelial cells and cardiomyocytes to cardiac EPHX2 expression, EET hydrolase activity, coronary artery vasodilation, and left ventricular function in isolated-perfused (Langendorff) hearts before/after I/R injury.

Results

Generation of mice and characterization of EPHX2 expression

Mice containing a conditional floxed (null) *Ephx2* allele (*Ephx2*$^{fx/fx}$) with *LoxP* sites flanking the fourth and fifth exons (Fig. 1*A*) were bred to transgenic mice with the *Cre* recombinase transgene driven by either the *Tek* or *Myh6* promoter to generate mice with disruption of *Ephx2* in endothelial cells or cardiomyocytes, respectively. After Cre recombination, exon 3 to exon 6 splicing would be expected to either result in a nonsense mutation and production of a truncated EPHX2 protein lacking the functional hydrolase domain, or alternatively, the EPHX2 protein produced from aberrant splicing would be rapidly degraded. *Ephx2*$^{fx/fx}$ *Cre* negative mice were used as WT controls. These mice were compared to conventional global *Ephx2*$^{-/-}$ mice that were previously generated (28). All mice were healthy, fertile, and survived to weaning in normal Mendelian ratios (Fig. 1*B*).

Cell-type selective disruption of *Ephx2* was confirmed by immunohistochemistry of heart, aorta, and kidney tissue sections. *Ephx2*$^{fx/fx}$ *Cre* negative (WT) mice predominately express EPHX2 in cardiomyocytes with lower level expression in some but not all heart endothelial cells (Fig. 2). Endothelial EPHX2 expression appeared mostly restricted to larger heart vessels rather than smaller arterioles or capillaries. EPHX2 staining was not observed in either heart smooth muscle cells or heart fibroblasts. EPHX2 was also expressed in endothelial cells in the aorta and kidney and in renal tubular epithelial cells. Importantly, *Ephx2*$^{fx/fx}$*/Tek-cre* tissues displayed selective loss of EPHX2 in endothelial cells of the heart, aorta, and kidney. In contrast, *Ephx2*$^{fx/fx}$*/Myh6-cre* hearts had selective loss of EPHX2 only in cardiomyocytes. Global *Ephx2* disruption abolished EPHX2 staining in all cell types (Fig. 2).

We quantified EPHX2 expression in hearts from each of the four mouse lines. *Ephx2* mRNA levels were not significantly reduced in *Ephx2*$^{fx/fx}$*/Tek-cre* hearts relative to *Ephx2*$^{fx/fx}$ *Cre* negative (WT) hearts. In contrast, both *Ephx2*$^{fx/fx}$*/Myh6-cre* and global *Ephx2*$^{-/-}$ hearts had significantly less *Ephx2* mRNA compared to both *Ephx2*$^{fx/fx}$ *Cre* negative and *Ephx2*$^{fx/fx}$*/Tek-cre* hearts. *Ephx1* expression was not different among the four genotypes (Fig. 3*A*). Based on these data, we can draw two conclusions: (1) Cre-induced recombination of the *Ephx2*$^{fx/fx}$ locus results in an unstable, rapidly degraded *Ephx2* mRNA and (2) the 93% reduction in *Ephx2* mRNA in *Ephx2*$^{fx/fx}$*/Myh6-cre* hearts suggests that the vast majority of cardiac *Ephx2* is expressed in cardiomyocytes. The mRNA data were independently corroborated by Western blot analysis. EPHX2 protein expression was similar in *Ephx2*$^{fx/fx}$ *Cre* negative and *Ephx2*$^{fx/fx}$*/Tek-cre* hearts but below the limit of detection in *Ephx2*$^{fx/fx}$*/Myh6-cre* and global *Ephx2*$^{-/-}$ hearts. No truncated or alternately spliced forms of EPHX2 were observed (Fig. 3*B*).

Characterization of cardiac EPHX2 activity in vitro and ex vivo

We quantified 14,15-EET hydrolysis rates *in vitro* in cardiac lysates from mice of each genotype. 14,15-EET hydrolysis was not significantly altered in *Ephx2*$^{fx/fx}$*/Tek-cre* heart lysates relative to *Ephx2*$^{fx/fx}$ *Cre* negative heart lysates. In contrast, *Ephx2*$^{fx/fx}$*/Myh6-cre* and global *Ephx2*$^{-/-}$ heart lysates showed 94% and 97% reduction in 14,15-EET hydrolysis rates relative to *Ephx2*$^{fx/fx}$ *Cre* negative heart lysates (Fig. 3*C*). Compared to *Ephx2*$^{fx/fx}$ *Cre* negative heart lysates, *Ephx2*$^{fx/fx}$*/Myh6-cre* heart lysates showed similar reductions in the rates of hydrolysis of 11,12-EET (95%), 12,13-EpOME (91%), 17,18-EpETE (84%),

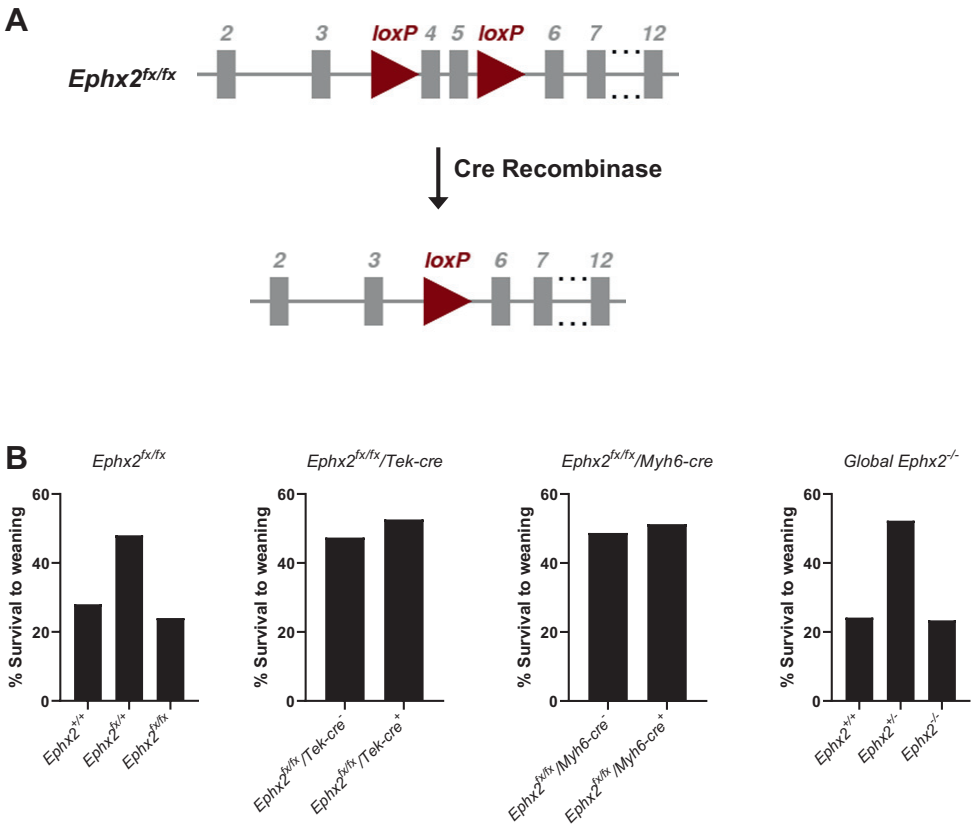

Figure 1. Schematic representation of the conditional null floxed *Ephx2* allele. *A*, *Ephx2*$^{fx/fx}$ mice contain insertions of loxP sites flanking the fourth and fifth exons of *Ephx2*. Following Cre recombination, loss of exons 4 and 5 might result in an unstable transcript or a frameshifted transcript containing a stop codon in exon 6. *B*, the percentage of pups genotyped at weaning for *Ephx2*$^{fx/fx}$, *Ephx2*$^{fx/fx}$*/Tek-cre*, *Ephx2*$^{fx/fx}$*/Myh6-cre*, and *global Ephx2*$^{-/-}$ mouse lines. None of the ratios were significantly different from normal Mendelian ratios. N = 304 to 503 pups per line, $p > 0.05$. EPHX, epoxide hydrolase.

and 19,20-EpDPE (88%) (Fig. 3*C*). These data suggest that ~90 to 95% of cardiac EPHX2 activity is in cardiomyocytes, with a small residual activity in endothelial cells.

Cell-type selective *Ephx2* disruption had similar effects on EET hydrolysis *ex vivo* in isolated-perfused hearts. Hearts were perfused in retrograde manner using the Langendorff method for 40 min (baseline), subjected to 20 min of global, no-flow ischemia, and then 40 min of reperfusion. Perfusates spilling out of the heart into the warming reservoir were collected during the last 20 min of baseline perfusion and the first 20 min of reperfusion, and EET and dihydroxyeicosatrienoic acid (DHET) levels were measured by LC/MS/MS. At baseline, there were no significant differences in cardiac generation of EETs or DHETs between the four genotypes (Fig. 4). Relative to baseline, levels of 14,15-EET and 14,15-DHET were increased during reperfusion in *Ephx2*$^{fx/fx}$ *Cre* negative and *Ephx2*$^{fx/fx}$*/Tek-cre* hearts (Fig. 4*A*). Hearts from both *Ephx2*$^{fx/fx}$*/Myh6-cre* and global *Ephx2*$^{-/-}$ mice also generated more 14,15-EET during reperfusion compared to baseline; however, both *Ephx2*$^{fx/fx}$*/Myh6-cre* and global *Ephx2*$^{-/-}$ hearts produced significantly less 14,15-DHET than *Ephx2*$^{fx/fx}$ *Cre* negative hearts during reperfusion. Interestingly, during reperfusion, 14,15-DHET levels from *Ephx2*$^{fx/fx}$*/Myh6-cre* hearts were slightly, albeit significantly higher than those from global *Ephx2*$^{-/-}$ hearts, which suggests a role for endothelial EPHX2 in 14,15-EET hydrolysis in postischemic hearts. Similar results were observed for cardiac perfusate 11,12-EET and 11,12-DHET levels (Fig. 4*B*), and 8,9-EET and 8,9-DHET levels (Fig. 4*C*). Since EPHX2 is most responsible for 14,15-EET hydrolysis *in vivo* (3), the 14,15-EET:DHET ratio typically reflects EPHX2 activity, with higher epoxide:diol ratios suggesting lower EPHX2 activity. During reperfusion, the 14,15-EET:DHET ratios in *Ephx2*$^{fx/fx}$ *Cre* negative (0.96 ± 0.11) and *Ephx2*$^{fx/fx}$*/Tek-cre* (1.16 ± 0.26) perfusates were not significantly changed; however, 14,15-EET:DHET ratios in *Ephx2*$^{fx/fx}$*/Myh6-cre* (1.43 ± 0.18) and global *Ephx2*$^{-/-}$ (2.4 ± 0.32) perfusates were significantly increased compared to *Ephx2*$^{fx/fx}$ *Cre* negative perfusates ($p < 0.05$). Notably, the 14,15-EET:DHET ratio in global *Ephx2*$^{-/-}$ perfusates was significantly higher than *Ephx2*$^{fx/fx}$*/Myh6-cre* perfusates, which suggests some contribution of nonmyocardial EPHX2 toward overall EPHX2 activity. Other fatty acid epoxides and diols showed a similar pattern of epoxide to diol hydrolysis *ex vivo* (Table 1).

Characterization of cardiac function at baseline and after I/R

To determine the effect of cell-selective *Ephx2* disruption on cardiac function and coronary flow, each of the four genotypes was evaluated in Langendorff isolated-perfused hearts. Heart

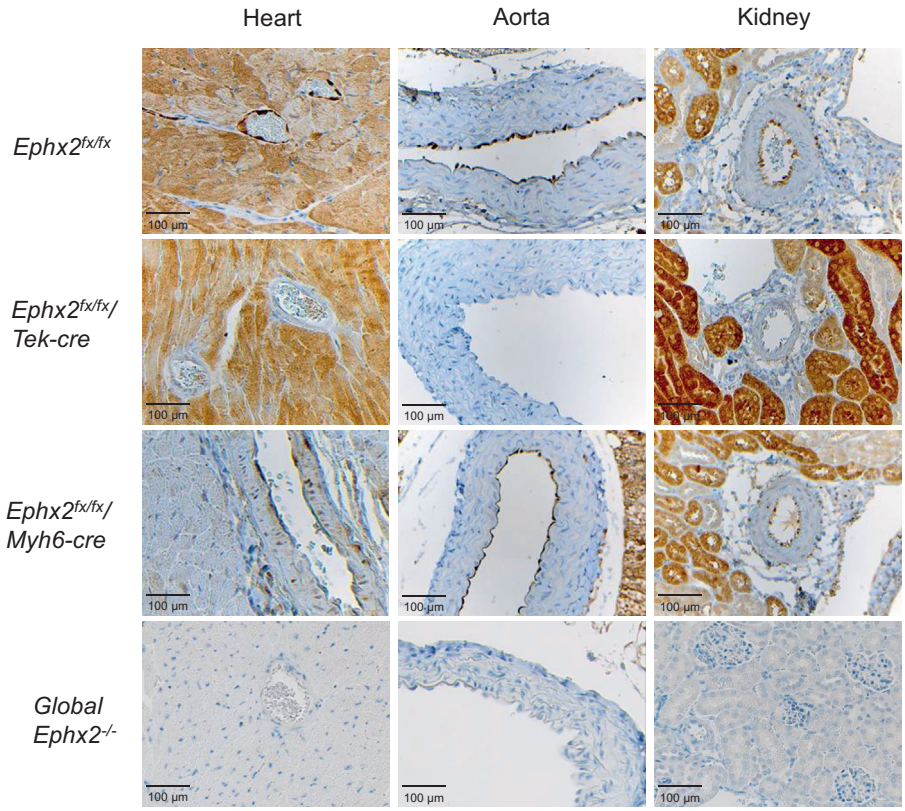

Figure 2. Immunohistochemical staining of EPHX2 in tissues from *Ephx2*$^{fx/fx}$ and *Ephx2*-deficient mice. Expression of EPHX2 in heart, aorta, and kidney from *Ephx2*$^{fx/fx}$ *Cre* negative, *Ephx2*$^{fx/fx}$/*Tek-cre*, *Ephx2*$^{fx/fx}$/*Myh6-cre*, and global *Ephx2*$^{-/-}$ mice was detected by immunohistochemistry using a selective EPHX2 antibody (sc-22344). Data are representative of at least three mice per genotype group. EPHX, epoxide hydrolase.

function was assessed during 40 min of baseline perfusion, 20 min of global, no-flow ischemia, and 40 min of reperfusion. Baseline characteristics, including heart rate, left ventricular developed pressure (LVDP), rate pressure product (RPP), dP/dt_{max}, dP/dt_{min}, time to ischemic contracture, and maximal ischemic contracture (C_{max}), are shown in Table 2. No significant changes were found in any of the baseline parameters between *Ephx*$^{fx/fx}$ *Cre* negative hearts and those of any of the three *Ephx2*-disrupted lines. *Ephx*$^{fx/fx}$ *Cre* negative hearts displayed similar functional recovery as WT hearts in previous experiments in our laboratory (24% ± 4% recovery of LVDP and 24% ± 6% recovery of RPP at R40) (3, 6, 29, 30). Functional recovery in *Ephx2*$^{fx/fx}$/*Tek-cre* hearts was not significantly different from *Ephx*$^{fx/fx}$ *Cre* negative hearts after I/R (22% ± 8% recovery of LVDP, 22% ± 9% recovery of RPP) (Fig. 5*A*). Similar to previous experiments (3, 6), global *Ephx2*$^{-/-}$ hearts had significantly increased recovery of LVDP and RPP after I/R compared to *Ephx*$^{fx/fx}$ *Cre* negative hearts (48% ± 4% recovery of LVDP, 45% ± 5% recovery of RPP, $p < 0.05$ *versus Ephx*$^{fx/fx}$). Interestingly, *Ephx2*$^{fx/fx}$/*Myh6-cre* cardiac functional recovery after I/R was significantly increased compared to *Ephx*$^{fx/fx}$ *Cre* negative hearts (42% ± 5% recovery of LVDP, 41% ± 5% recovery of RPP, $p < 0.05$ *versus Ephx*$^{fx/fx}$) (Fig. 5*A*). Thus, postischemic functional recovery in *Ephx2*$^{fx/fx}$/*Myh6-cre* hearts was comparable to that in global *Ephx2*$^{-/-}$ hearts.

The improvement in postischemic functional recovery in mice with global or myocardial disruption of *Ephx2* correlates with reduction in the hydrolysis of several EpFAs. The improvement could be due to reduced hydrolysis of beneficial EETs, or reduced formation of deleterious DiHOMEs, which have vasoconstrictive and cardiodepressive effects (29). To date, there are no known inhibitors of DiHOME function; however, 14,15-epoxyeicosa-5(Z)-enoic acid (EEZE) acts as a selective EET antagonist (31). To distinguish between these two possibilities, we treated hearts with either EEZE or vehicle and examined LVDP and RPP recovery after ischemia. Vehicle-treated *Ephx2*$^{fx/fx}$/*Myh6-cre* hearts again showed significantly improved recovery of function compared to vehicle-treated *Ephx*$^{fx/fx}$ *Cre* negative hearts (61% ± 7% *versus* 29% ± 1% recovery of LVDP, 55% ± 5% *versus* 30% ± 10% recovery of RPP, respectively $p < 0.05$). Treatment of hearts with EEZE significantly reduced the recovery of LVDP in both *Ephx2*$^{fx/fx}$/*Myh6-cre* and *Ephx*$^{fx/fx}$ *Cre* negative hearts (16% ± 2% and 12% ± 2% recovery of LVDP, 17% ± 3% and 11% ± 2% recovery of RPP, respectively, $p < 0.05$ *versus* vehicle for both genotypes). These data strongly suggest that the improved recovery of myocardial function in *Ephx2*$^{fx/fx}$/*Myh6-cre* hearts is due to the reduced hydrolysis of beneficial EETs, rather than a reduction in cardiodepressive DiHOMEs.

Hearts with myocardial-selective disruption of *Ephx2* exhibited increased activation of ERK signaling during postischemic reperfusion and this effect was EET-dependent. ERK phosphorylation/activation was low in basal functioning hearts independent of genotype (Fig. 6, *A* and *B*, unpublished observations). ERK was activated in *Ephx2*$^{fx/fx}$ *Cre* negative hearts 10 min after the onset of reperfusion. Remarkably, ERK

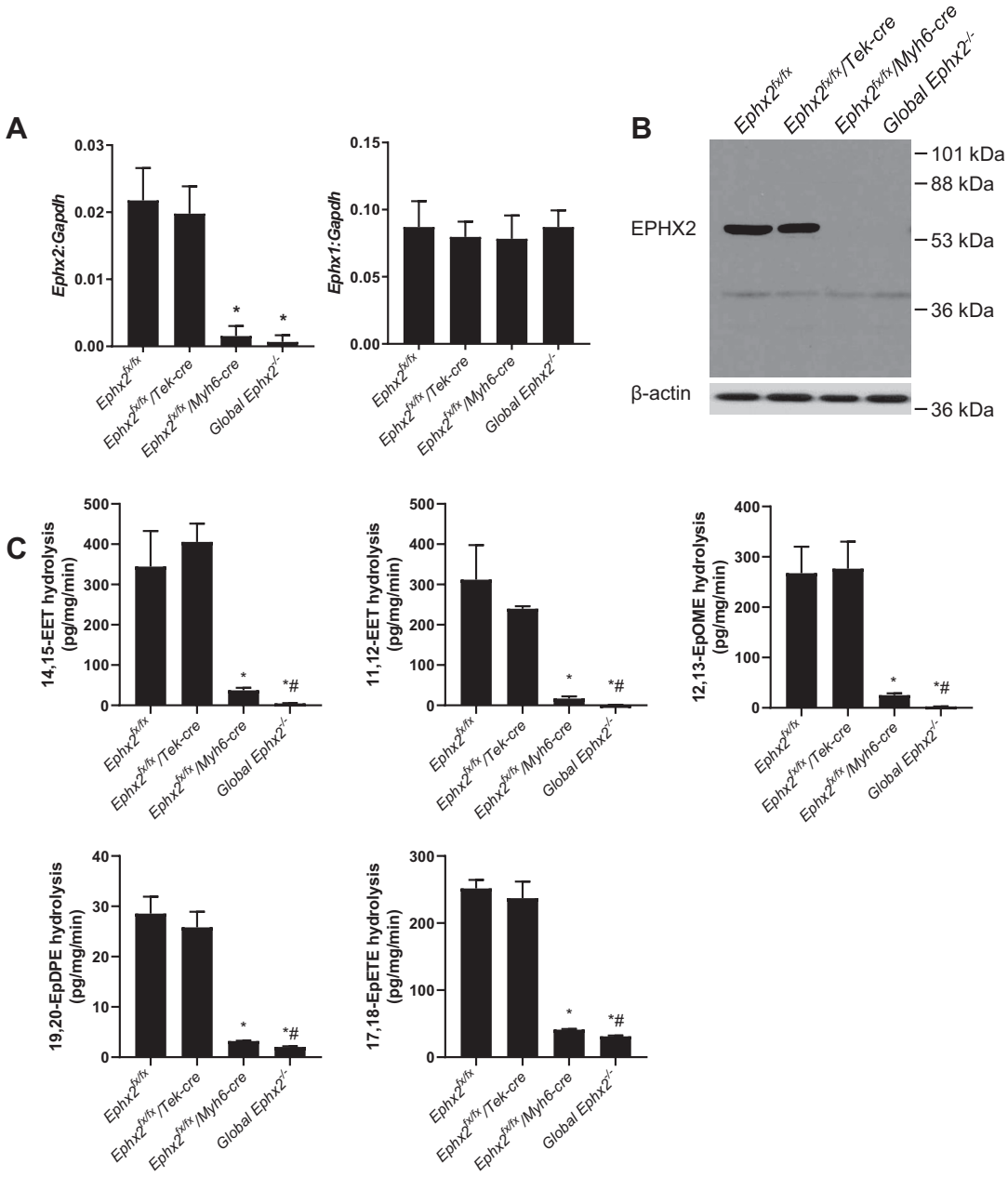

Figure 3. EPHX2 expression in hearts from *Ephx2*$^{fx/fx}$ and *Ephx2*-deficient mice. *A*, mRNA levels as determined by real-time, quantitative RT-PCR analysis in hearts from *Ephx2*$^{fx/fx}$ *Cre* negative, *Ephx2*$^{fx/fx}$*/Tek-cre*, *Ephx2*$^{fx/fx}$*/Myh6-cre*, and global *Ephx2*$^{-/-}$ mice. Data are expressed as arbitrary units. N = 4 to 6 mice/group, *$p < 0.05$ *versus Ephx2*$^{fx/fx}$. *B*, representative Western blot of *Ephx2*$^{fx/fx}$ *Cre* negative, *Ephx2*$^{fx/fx}$*/Tek-cre*, *Ephx2*$^{fx/fx}$*/Myh6-cre*, and global *Ephx2*$^{-/-}$ heart lysates sequentially probed with EPHX2 and β-actin antibodies. *C*, rate of hydrolysis of 14,15-EET, 11,12-EET, 12,13-EpOME, 19,20-EpDPE, and 17,18-EpETE in *Ephx2*$^{fx/fx}$ *Cre* negative, *Ephx2*$^{fx/fx}$*/Tek-cre*, *Ephx2*$^{fx/fx}$*/Myh6-cre*, and global *Ephx2*$^{-/-}$ heart lysates expressed in pg/mg protein/min. N = 4 mice per group, *$p <$ 0.05 *versus Ephx2*$^{fx/fx}$. EET, epoxyeicosatrienoic acid; EPHX, epoxide hydrolase; EpDPE, epoxydocosapentaenoic acid; EpETE, epoxyeicosatetraenoic acid.

activation was significantly higher in *Ephx2*$^{fx/fx}$*/Myh6-cre* hearts than in *Ephx2*$^{fx/fx}$ *Cre* negative hearts (Fig. 6, *A* and *B*, $p < 0.05$). The strong activation of ERK in *Ephx2*$^{fx/fx}$*/Myh6-cre* hearts was significantly attenuated by pretreatment with EEZE (Fig. 6, *A* and *B*, $p < 0.05$), suggesting that the genotype differences in ERK activation were mediated by EETs. GSK3β phosphorylation followed a similar pattern as that observed for ERK phosphorylation although the differences were not statistically significant (Fig. 6, *C* and *D*). Together, these data suggest that disruption of *Ephx2* in cardiomyocytes is sufficient to change global activation of signaling pathways in the heart.

Dysregulation of EpFA metabolism can significantly regulate vascular flow in isolated-perfused hearts (29). To determine if selective Ephx2 disruption regulates vascular perfusion in isolated hearts, coronary flow rates were measured at baseline and throughout the first 20 min of postischemic reperfusion in noninstrumented hearts. None of the three *Ephx2*-disrupted genotypes were significantly different from *Ephx*$^{fx/fx}$ *Cre* negative hearts at baseline or throughout the 20 min of recovery after ischemia (Fig. 7). Thus, EPHX2-mediated EpFA hydrolysis does not significantly regulate coronary flow at baseline or after 20 min of global, no-flow

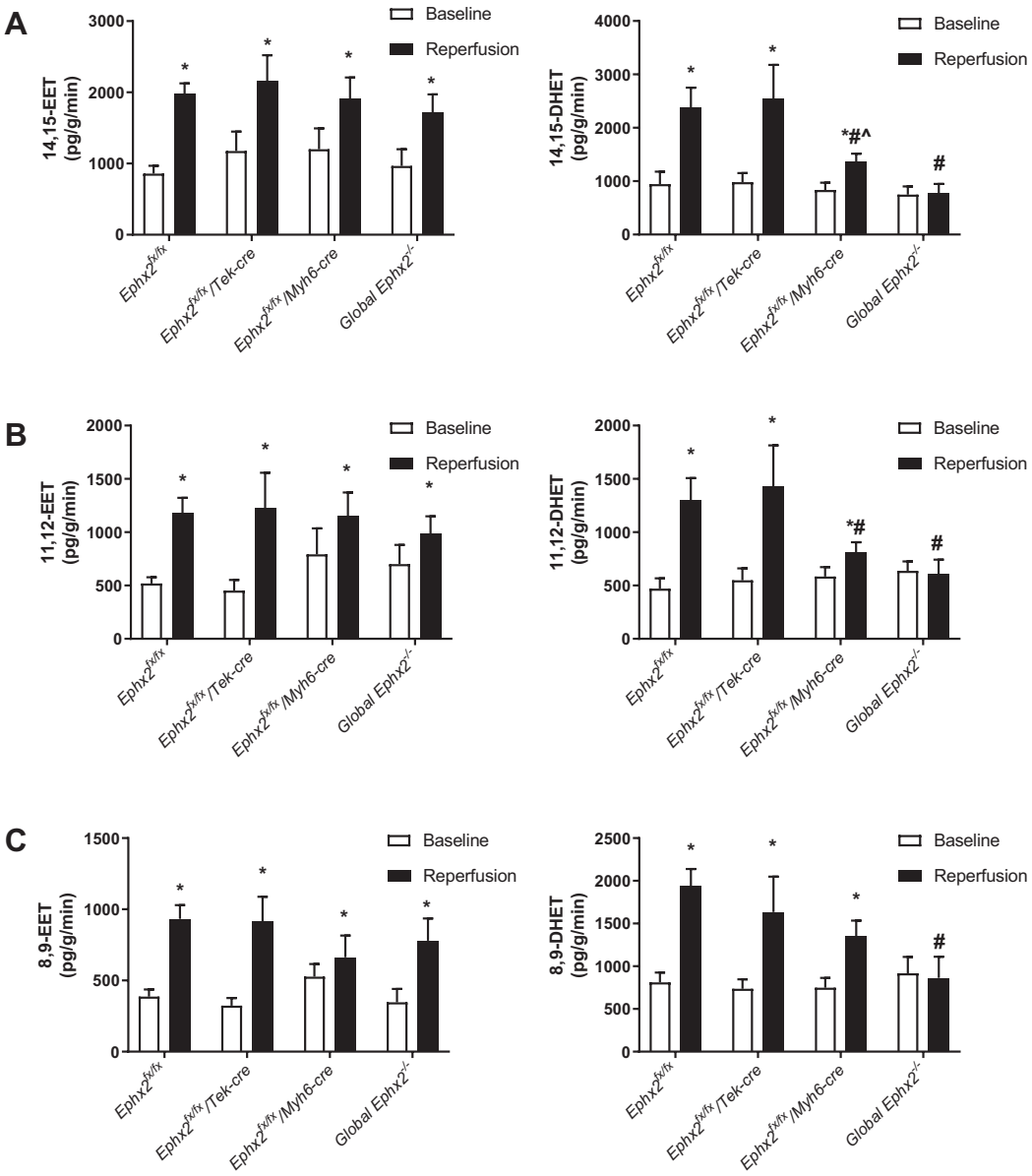

Figure 4. Levels of EETs and DHETs in Langendorff heart perfusates before and after ischemia. Cardiac perfusates were collected during the last 20 min of baseline and the first 20 min of reperfusion; EET and DHET levels were measured by LC/MS/MS. Levels of (*A*) 14,15-EET and DHET, (*B*) 11,12-EET and DHET, or (*C*) 8,9-EET and DHET released from *Ephx2*$^{fx/fx}$ *Cre* negative, *Ephx2*$^{fx/fx}$*/Tek-cre*, *Ephx2*$^{fx/fx}$*/Myh6-cre*, and global *Ephx2*$^{-/-}$ hearts before and after ischemia are displayed as pg/gram of heart tissue/min. N = 5 to 10 mice per group, *$p < 0.05$ *versus* baseline of same genotype, ^$p < 0.05$ *versus Ephx2*$^{-/-}$, #$p < 0.05$ *versus Ephx2*$^{fx/fx}$. DHET, dihydroxyeicosatrienoic acid; EET, epoxyeicosatrienoic acid; EPHX, epoxide hydrolase.

ischemia. Taken together, these data suggest that EPHX2 expression in cardiomyocytes, but not endothelial cells, regulates postischemic recovery of heart function, but not coronary flow.

Discussion

The potent cardioprotective effects of EETs are diminished after hydrolysis by EPHXs such as EPHX2. Genetic disruption or pharmacological inhibition of EPHX2 improves postischemic recovery of heart function and suggests a promising role for EPHX2 inhibitors for the treatment of myocardial infarction (5, 6). Herein, we describe the development and characterization of two novel mouse models with cell-selective *Ephx2* genetic disruption and provide evidence for cell-specific physiological roles of EPHX2-mediated EET hydrolysis in the heart. Our major findings include the following: (1) immunohistochemical staining revealed that cardiac EPHX2 is expressed abundantly in cardiomyocytes with some EPHX2 expression in endothelial cells surrounding large vessels; no EPHX2 staining was observed in cardiac smooth muscle cells or fibroblasts; (2) quantitative PCR and Western blot experiments indicate that ∼95% of cardiac EPHX2 is expressed in cardiomyocytes; (3) EPHX2 in cardiomyocytes, but not endothelial cells, is primarily responsible for hydrolysis of EETs in the heart *in vitro* and *ex vivo*; (4) EPHX2 in cardiomyocytes, but not endothelial cells, is responsible for improved postischemic functional recovery in the heart; (5) disruption of

Table 1
Fatty acid levels in Langendorff heart perfusates before and after ischemia

	Baseline				Reperfusion			
Oxylipins	*Ephx2*$^{fx/fx}$	*Ephx2*$^{fx/fx}$/*Tek-Cre*	*Ephx2*$^{fx/fx}$/*Myh6-Cre*	*Ephx2*$^{-/-}$	*Ephx2*$^{fx/fx}$	*Ephx2*$^{fx/fx}$/*Tek-Cre*	*Ephx2*$^{fx/fx}$/*Myh6-Cre*	*Ephx2*$^{-/-}$
n	10	7	7	5	10	7	7	5
6-keto-$PGF_{1\alpha}$	47.7 ± 9	49.3 ± 11.2	43.7 ± 10.3	51.4 ± 10.7	73.7 ± 10.7[a]	96.8 ± 13.5[a]	76.2 ± 8.6[a]	57.4 ± 18.3[a]
TXB_2	3.1 ± 0.5	3.6 ± 0.4	4.8 ± 2.5	3.4 ± 0.2	11.4 ± 1.8[a]	13 ± 1.8[a]	8.4 ± 0.8[a]	6.6 ± 2.3[a]
$PGF_{2\alpha}$	3.2 ± 0.4	3 ± 0.4	3.4 ± 0.8	3.6 ± 0.5	6 ± 0.7[a]	5.9 ± 0.4[a]	5.8 ± 0.4[a]	4.9 ± 2[a]
PGD_2	26.9 ± 5.1	26.6 ± 3.5	21.2 ± 5.4	26.9 ± 3.5	86.6 ± 9[a]	93 ± 5.6[a]	55.2 ± 5.6[a]	54.3 ± 18.7[a]
PGE_2	4.2 ± 0.7	5.1 ± 1.1	4.6 ± 1.3	3.2 ± 0.7	7.8 ± 1[a]	8.9 ± 1.2[a]	9.6 ± 1.9[a]	4.8 ± 1.9[a]
8-iso-$PGF_{2\alpha}$	0.26 ± 0.04	0.27 ± 0.02	0.22 ± 0.06	0.23 ± 0.02	0.52 ± 0.07[a]	0.56 ± 0.08[a]	0.42 ± 0.03[a]	0.39 ± 0.14[a]
14,15-EET	0.86 ± 0.11	1.18 ± 0.27	0.91 ± 0.11	0.97 ± 0.23	1.98 ± 0.14[a]	2.16 ± 0.3[a]	1.91 ± 0.3[a]	1.72 ± 0.26[a]
11,12-EET	0.52 ± 0.06	0.45 ± 0.1	0.82 ± 0.28	0.7 ± 0.18	1.18 ± 0.14[a]	1.23 ± 0.33[a]	1.15 ± 0.23[a]	0.98 ± 0.17[a]
8,9-EET	0.39 ± 0.05	0.32 ± 0.05	0.53 ± 0.09	0.35 ± 0.1	0.93 ± 0.1[a]	0.91 ± 0.17[a]	0.66 ± 0.15[a]	0.78 ± 0.16[a]
5,6-EET	ND	ND	ND	ND	ND	ND	ND	ND
14,15-DHET	0.94 ± 0.23	0.98 ± 0.17	0.84 ± 0.14	0.75 ± 0.15	2.38 ± 0.37[a]	2.55 ± 0.63[a]	1.37 ± 0.18[abc]	0.77 ± 0.18[ac]
11,12-DHET	0.47 ± 0.1	0.55 ± 0.11	0.58 ± 0.09	0.64 ± 0.21	1.3 ± 0.21[a]	1.43 ± 0.39[a]	0.81 ± 0.09[a]	0.61 ± 0.13[c]
8,9-DHET	0.81 ± 0.11	0.74 ± 0.11	0.75 ± 0.11	0.92 ± 0.19	1.94 ± 0.41[a]	1.63 ± 0.41[a]	1.35 ± 0.18[a]	0.86 ± 0.25[c]
5,6-DHET	1.6 ± 0.13	1.7 ± 0.26	3.4 ± 1.1	1.25 ± 0.51	4.29 ± 0.51[a]	3.14 ± 0.8[a]	3.71 ± 0.86[a]	2.1 ± 0.44[ac]
12,13-EpOME	18.9 ± 3.1	11 ± 3.4	22.7 ± 6.7	12.4 ± 2.2	19.7 ± 4.1	16.3 ± 4.1	26.4 ± 8	20.8 ± 3.7[a]
9,10-EpOME	16.8 ± 3.8	13.3 ± 3	15.1 ± 11.6	15 ± 4.3	22.5 ± 2.2[a]	18.8 ± 4.8	27.8 ± 5.4[a]	23.2 ± 5.4[a]
12,13-DiHOME	11.1 ± 2	11.6 ± 1.6	11.5 ± 0.6	8.9 ± 1.9	35.9 ± 5.1[a]	33.1 ± 5.1[a]	25.8 ± 4.5[abc]	10.5 ± 2.2[c]
9,10-DiHOME	11 ± 2.9	5.2 ± 0.9	10 ± 3.4	7.3 ± 1.8	18.6 ± 2.8[a]	13.4 ± 3.6[a]	12 ± 3.6[ab]	5.1 ± 1.4[ac]
19,20-EpDPE	2.8 ± 0.6	2.6 ± 0.6	2.7 ± 0.5	2 ± 1.1	7 ± 1.1[a]	5.7 ± 1.1[a]	5.6 ± 1.1[a]	5.9 ± 1.2[a]
19,20-DiHDPA	9.2 ± 4.4	7.5 ± 1.8	6.5 ± 1.3	7 ± 1.4	17.2 ± 2.5[a]	17.2 ± 4.6[a]	10.3 ± 1.4[ac]	6.7 ± 2.3[c]
17,18-EpETE	BD	BD	BD	BD	BD	BD	BD	BD
17,18-DiHETE	2.9 ± 0.52	3.4 ± 0.6	3.0 ± 0.8	3.4 ± 1.4	9.4 ± 1.4[a]	9.2 ± 1.3[a]	5.3 ± 0.9[ac]	3.2 ± 0.6[ac]
20-HETE	BD	BD	BD	BD	BD	BD	BD	BD
19-HETE	BD	BD	BD	BD	BD	BD	BD	BD
15-HETE	6 ± 0.6	5.1 ± 1	5 ± 1.6	5.6 ± 1.1	11.8 ± 1.1[a]	12.4 ± 1.2[a]	14.8 ± 2.8[a]	11.5 ± 2.8[a]
12-HETE	78 ± 14	76 ± 16	76 ± 14	91 ± 30	134 ± 27[a]	113 ± 27[a]	135 ± 16[a]	127 ± 14[a]
11-HETE	3.7 ± 0.5	3.3 ± 0.6	5.6 ± 1.3	3.3 ± 1	8.4 ± 1[a]	6.5 ± 0.8[a]	10.4 ± 3[a]	6.2 ± 1.8[a]
8-HETE	37 ± 5	31 ± 6	38 ± 5	39 ± 11	103 ± 11[a]	97 ± 6[a]	131 ± 36[a]	90 ± 8[a]
5-HETE	2.5 ± 0.3	2.5 ± 0.6	3.4 ± 0.6	2.4 ± 0.4	9.7 ± 1[a]	9.1 ± 1.3[a]	9.7 ± 2.1[a]	6.7 ± 2[a]
13-HODE	96 ± 23	97 ± 16	92 ± 13	80 ± 12	169 ± 14[a]	205 ± 24[a]	209 ± 16[a]	165 ± 28[a]
9-HODE	55 ± 9	59 ± 12	104 ± 36	63 ± 14	123 ± 24[a]	122 ± 18[a]	108 ± 18[a]	105 ± 17[a]
14,15-EET:DHET	1.12 ± 0.16	1.29 ± 0.19	1.33 ± 0.34	1.37 ± 0.11	0.96 ± 0.11	1.16 ± 0.26	1.43 ± 0.18[bc]	2.4 ± 0.32[ac]
11,12-EET:DHET	1.42 ± 0.25	0.88 ± 0.15	1.59 ± 0.46	1.06 ± 0.22	1.05 ± 0.17	1.01 ± 0.17	1.42 ± 0.23	1.8 ± 0.35[c]
8,9-EET:DHET	0.48 ± 0.04	0.43 ± 0.05	0.71 ± 0.12[a]	0.38 ± 0.09	0.48 ± 0.06	0.56 ± 0.08	0.49 ± 0.09	0.91 ± 0.10[c]
12,13-EpOME:DiHOME	1.11 ± 0.17	0.94 ± 0.15	1.31 ± 0.28	0.94 ± 0.18	0.63 ± 0.09[a]	0.84 ± 0.22	1.58 ± 0.3[c]	2.2 ± 0.48[ac]
9,10-EpOME:DiHOME	2.58 ± 0.33	2.69 ± 0.5	5.06 ± 1.44	2.26 ± 0.49	1.43 ± 0.16[a]	1.74 ± 0.44	3.71 ± 0.62[c]	6.51 ± 2.90[ac]
19,20-EpDPE:DiHDPA	0.45 ± 0.06	0.39 ± 0.07	0.48 ± 0.14	0.31 ± 0.06	0.45 ± 0.07	0.46 ± 0.12	0.49 ± 0.08	0.63 ± 0.13

Cardiac perfusates were collected during the last 20 min of baseline and the first 20 min of reperfusion and assayed for oxylipins by LC/MS/MS. Levels of oxylipins are shown in ng/g/min (mean ± SEM). 11,12- and 14,15-EET:DHET ratios are mean ± SEM of individual values. N = 5 to 10 mice/group as indicated.
Abbreviations: BD, below detection; ND, not determined.
[a] $p < 0.05$ *versus* baseline of same genotype.
[b] $p < 0.05$ *versus* global *Ephx2*$^{-/-}$.
[c] $p < 0.05$ *versus* *Ephx2*$^{fx/fx}$ *Cre* negative.

Ephx2 in cardiomyocytes increase ERK activation after ischemia; (6) *Ephx2* disruption improves cardiac functional recovery through reduction of EET hydrolysis; and (7) neither EPHX2 in cardiomyocytes nor EPHX2 in endothelial cells regulates coronary flow before or after I/R.

Immunohistochemical staining revealed that EPHX2 is abundantly expressed in cardiomyocytes in the heart. This confirms previous reports that EPHX2 is expressed in the heart (6) and in "myocardium" and "blood vessels" of the cardiovascular system (10). Interestingly, our immunohistochemical staining suggests that endothelial expression was mostly restricted to larger blood vessels rather than endothelial cells of smaller vessels/arterioles or capillaries. We did, however, consistently observe endothelial expression of EPHX2 in aorta and renal arterioles. Our data is insufficient to determine the relative expression of EPHX2 in

Table 2
Baseline cardiac parameters in Langendorff ischemia/reperfusion studies

Parameter	*Ephx2*$^{fx/fx}$	*Ephx2*$^{fx/fx}$/*Tek-Cre*	*Ephx2*$^{fx/fx}$/*Myh6-Cre*	*Ephx2*$^{-/-}$
n	9	6	9	6
Heart rate (beats/min)	347 ± 16	360 ± 27	357 ± 8	366 ± 4
LVDP (cmH_2O)	114 ± 6	109 ± 11	120 ± 4	117 ± 6
RPP (cmH_2O/min)	39900 ± 3600	39500 ± 5500	42700 ± 1900	42900 ± 2200
dP/dt_{max} (cmH_2O/s)	5780 ± 230	6050 ± 540	6160 ± 250	5290 ± 210
dP/dt_{min} (cmH_2O/s)	−3420 ± 170	−3850 ± 560	−3510 ± 160	−3060 ± 180
TIC (min)	5.9 ± 0.3	5.6 ± 0.2	5.5 ± 0.3	5.8 ± 0.3
C_{max} (cmH_2O)	110 ± 7	108 ± 3	104 ± 4	104 ± 6

All values mean ± SEM.
Abbreviations: C_{max}, Maximum contracture; dP/dt_{max}, rate of maximal contraction; dP/dt_{min}, rate of minimal contraction; LVDP, Left Ventricular Developed Pressure; RPP, Rate-Pressure Product; TIC, Time to Ischemic Contracture.

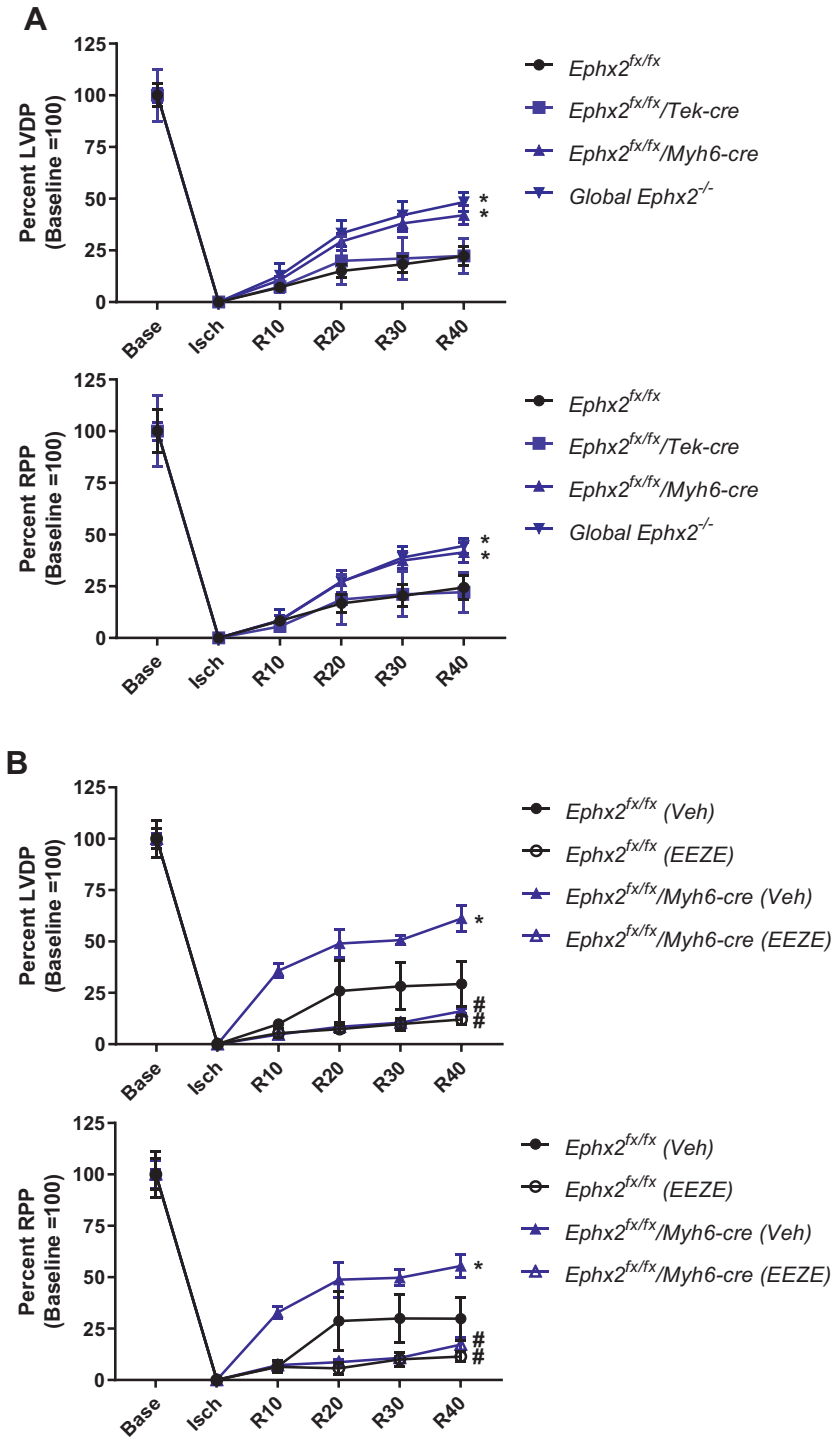

Figure 5. Recovery of cardiac contractile function during reperfusion after ischemia in *Ephx2*$^{fx/fx}$ and *Ephx2*-deficient hearts. Recovery of (*A*) left ventricular developed pressure (LVDP) or Rate Pressure Product (RPP) by *Ephx2*$^{fx/fx}$ *Cre* negative, *Ephx2*$^{fx/fx}$*/Tek-cre*, *Ephx2*$^{fx/fx}$*/Myh6-cre*, and global *Ephx2*$^{-/-}$ hearts is expressed as a percentage of baseline values. N = 6 to 9 mice per group, *$p < 0.05$ *versus Ephx2*$^{fx/fx}$. *B*, recovery of LVDP or RPP by *Ephx2*$^{fx/fx}$ *Cre* negative or *Ephx2*$^{fx/fx}$*/Myh6-cre* hearts after treatment with ethanol vehicle (Veh) or 1 μM EEZE. N = 4 mice per group, *$p < 0.05$ *versus Ephx2*$^{fx/fx}$, #$p < 0.05$ *versus* Vehicle. EEZE, 14,15-epoxyeicosa-5(Z)-enoic acid; EPHX, epoxide hydrolase.

cardiomyocytes or endothelial cells; the larger cardiomyocytes exhibited broad diffuse staining, while the smaller endothelial cells that expressed EPHX2 exhibited more intense cytoplasmic staining. Our data appears consistent with Human Protein Atlas single cell RNA data which suggests that cardiomyocytes express approximately three times as much *EPHX2* mRNA as endothelial cells (https://www.proteinatlas.org/ENSG00000120915-EPHX2).

Contrary to a previous report (12), which observed strong EPHX2 staining in human vascular smooth muscle cells, we did not observe murine EPHX2 expression in smooth muscle cells in any organs analyzed. It is possible that humans express

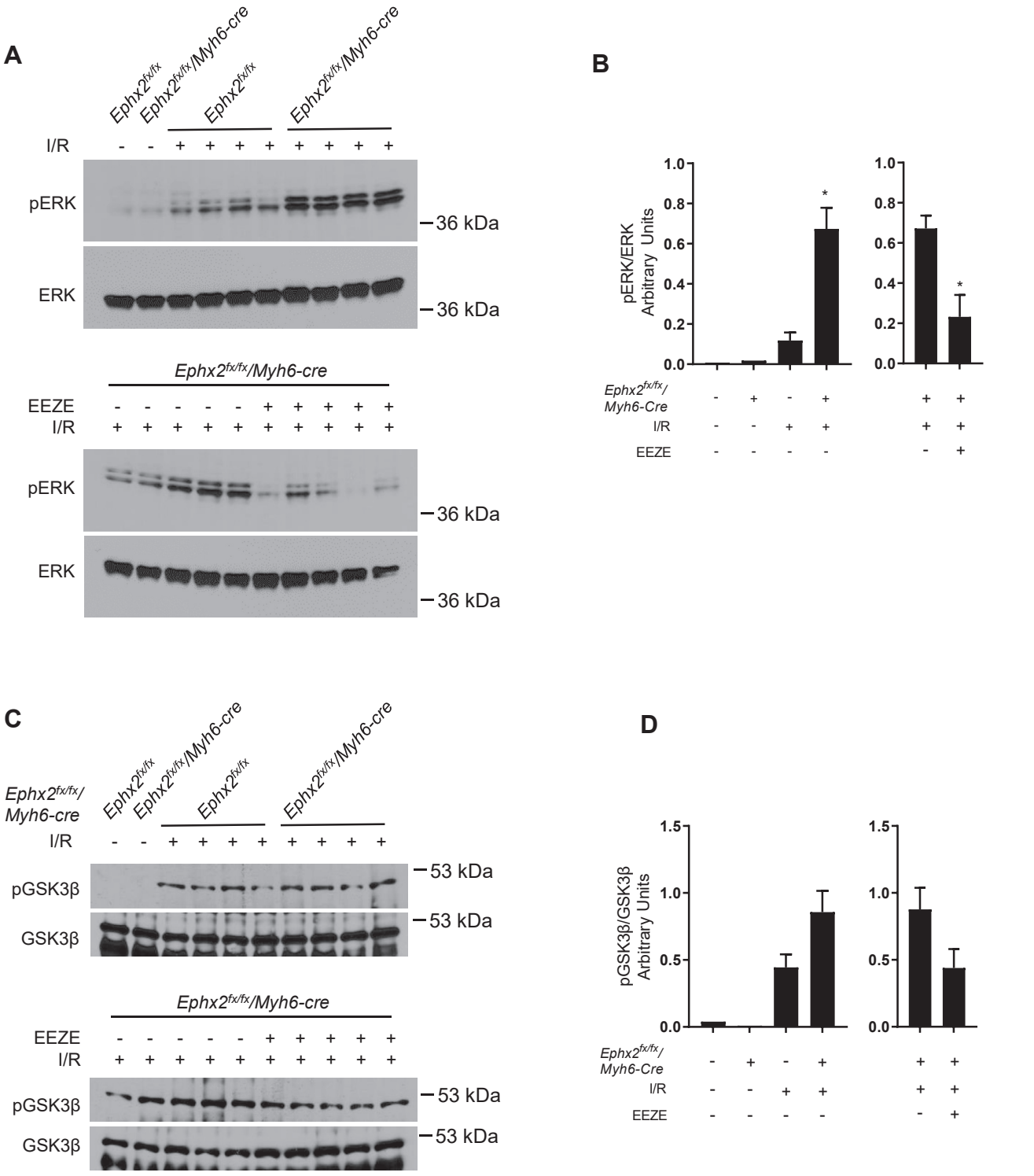

Figure 6. Regulation of ERK and GSK3β phosphorylation during reperfusion after ischemia in *Ephx2*$^{fx/fx}$ and *Ephx2*$^{fx/fx}$*/Myh6-cre* hearts treated with vehicle or EEZE. Detection and densitometric quantification of pERK and total ERK (*A* and *B*) or pGSK3β and total GSK3β (*C* and *D*) in *Ephx2*$^{fx/fx}$ *Cre* negative and *Ephx2*$^{fx/fx}$*/Myh6-cre* heart lysates obtained under basal (nonischemic) conditions or after ischemia and 10 min of reperfusion, with or without ethanol vehicle or 1 μM EEZE pretreatment as indicated. N = 1 (non-ischemic) or N = 4 to 5 (I/R) as indicated, *$p < 0.05$ *versus* *Ephx2*$^{fx/fx}$ or vehicle. EEZE, 14,15-epoxyeicosa-5(Z)-enoic acid; EPHX, epoxide hydrolase; I/R, ischemia/reperfusion.

EPHX2 in vascular smooth muscle or that factors such as age and/or inflammatory status of samples may induce EPHX2 expression in these cells. Coronary fibroblasts, which comprise approximately 15% of cardiac cells (7, 8), also did not appear to express appreciable EPHX2. The absence of staining in global *Ephx2*$^{-/-}$ tissues leads us to conclude with high confidence that our immunohistochemistry results accurately reflect the cellular distribution of murine EPHX2 expression. Importantly, our immunohistochemical analysis was independently confirmed by both qPCR, Western blot, and kinetic analysis;

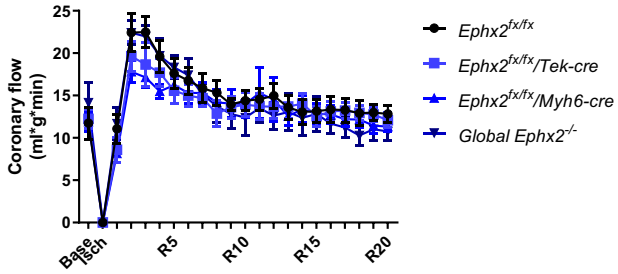

Figure 7. Coronary flow at baseline and during reperfusion after ischemia in *Ephx2*$^{fx/fx}$ and *Ephx2*-deficient hearts. Coronary perfusate flow was measured for each minute of perfusion at the end of baseline and for the first 20 min of reperfusion in *Ephx2*$^{fx/fx}$ *Cre* negative, *Ephx2*$^{fx/fx}$*/Tek-cre*, *Ephx2*$^{fx/fx}$*/Myh6-cre*, and global *Ephx2*$^{-/-}$ hearts. N = 4 to 9 mice per group. EPHX, epoxide hydrolase.

EPHX2 expression in *Ephx2*$^{fx/fx}$*/Tek-cre* hearts was largely unchanged relative to WT, whereas cardiomyocyte *Ephx2* disruption greatly reduced EPHX2 expression and activity to levels that were comparable to those in the global *Ephx2*-deficient mice.

Ischemia increased the production or release of all COX-, LOX- and P450-derived eicosanoids by 2- to 3-fold. Eicosanoid-synthetic enzymes such as COX2 and ALOX12 are not induced by short periods of cardiac ischemia and reperfusion (32, 33). Consistent, pathway-independent increases suggest that common, upstream activation of $iPLA_2$ and/or $cPLA_2$ isoforms released arachidonic acid to induce *de novo* formation of fatty acid epoxides, hydroxyls, and prostaglandins (34–36). Alternatively, some eicosanoids, including EETs, are stored esterified in membrane phospholipids and may be directly released by ischemia-activated PLA_2 (37, 38). Interestingly, hearts from all four genotype groups showed comparable levels of EETs and DHETs at baseline. These data suggest a substantial role for EPHX1 in EET hydrolysis at low basal rates of EET formation (3). Both global and cardiomyocyte-selective disruption of *Ephx2* reduced EET hydrolysis *in vitro* and *ex vivo* in working hearts. After ischemia, production of EETs and DHETs from hearts increased several-fold in WT control and endothelial-selective *Ephx2* null hearts; however, in cardiomyocyte-selective and global *Ephx2* null hearts, postischemic DHET production was significantly lower than in WT hearts. Importantly, in global *Ephx2* null hearts, postischemic DHET formation was similar to pre-ischemia baseline, which is consistent with the recently proposed concept that basal EET hydrolysis is mediated primarily by EPHX1, not EPHX2 (3, 39). EET levels increased in cardiomyocyte-selective and global *Ephx2* null hearts after ischemia to levels that were comparable to those in post-ischemic WT hearts. This seemingly enigmatic lack of increased EET levels in *Ephx2*-disrupted hearts is consistent with our previous findings (3) and suggests shunting to other pathways for EET metabolism that are reported to occur upon loss of EPHX2-mediated hydrolysis (1, 40, 41). In particular, increased reesterification of EETs is known to occur in cells when EET hydrolysis is inhibited (1, 40). Alternate pathways may include conversion of EETs to chain-shortened fatty acid epoxides that maintain at least some biological activity (42). Cardiomyocyte-selective *Ephx2* disruption enhanced the activation of cardioprotective ERK signaling after ischemia. Importantly, the improved ERK activation and recovery of function in hearts with myocardial *Ephx2* disruption was reversed with the selective EET antagonist EEZE, which suggests that reduced EPHX2-mediated EET hydrolysis was critical to recovery of function in these hearts.

Reduced hydrolysis of LA-, EPA-, and DHA-derived epoxides in hearts from mice with global or myocardial disruption of *Ephx2* may also improve cardiac function after ischemia. Hydrolysis of LA-derived EpOMEs (also called leukotoxins) activates them to more toxic DiHOMEs that induce vasoconstriction and impair ventricular contraction (29, 43, 44). The EPA- and DHA-derived epoxides are potently vasodilatory, anti-inflammatory, and anti-arrhythmic (45). While these mice are on an NIH31 diet that has a low omega-3:omega-6 ratio of 1:9.5 (Table S1), mouse hearts produce 5 to 10 times as much omega-3 EpFAs as EETs (Table 1). Nonetheless, the improvement in myocardial function after I/R in hearts with myocardial *Ephx2* disruption was completely reversed by the EET antagonist, 14,15-EEZE. Since EEZE does not block signaling by LA-, EPA-, or DHA-derived EpFAs (46), it appears that EETs are the main EPHX2-regulated EpFA involved in recovery of heart function on this diet in our model. We cannot not rule out that EPHX2 regulation of other EpFAs does not contribute, at least in part, to the development of cardiovascular disease or the postischemic recovery of heart function *in vivo*. The combination of omega-3 supplementation and EPHX2 inhibition may synergistically improve I/R recovery, as it does for other cardiovascular outcomes (47).

In this study, hearts with cardiomyocyte-specific disruption of *Ephx2* recapitulated nearly every phenotype of the global *Ephx2* null hearts. In particular, *Ephx2*$^{fx/fx}$*/Myh6-cre* hearts had similar recovery of function after ischemia as global *Ephx2*$^{-/-}$ hearts. Previous studies revealed that global *Ephx2*$^{-/-}$ hearts have increased PI3K activation and elevated GSK-3β phosphorylation that maintains mitochondrial integrity after ischemia (6). The fact that *Ephx2*$^{fx/fx}$*/Myh6-cre* hearts had similar postischemic functional recovery as global *Ephx2*$^{-/-}$ hearts suggests that the role of EPHX2 in EET hydrolysis and suppression of cardiac recovery largely occurs within cardiomyocytes, not other cardiac cell types. This result is consistent with previous data from our group which showed improved postischemic recovery of function in hearts with cardiomyocyte-specific transgenic overexpression of CYP2J2 but not in hearts with transgenic endothelial CYP2J2 overexpression (29). Together, these studies suggest the importance of cellular compartmentalization of EET formation and hydrolysis in the heart.

Somewhat surprisingly, we did not observe the regulation of coronary vascular tone by EPHX2 *ex vivo* at baseline or during I/R. Inhibition or genetic disruption of EPHX2 would be expected to increase the local production of EETs and promote vasodilation (9, 48). We did not observe increased coronary vasodilation in any of the *Ephx2*-disrupted models relative to *Ephx2*$^{fx/fx}$ *Cre* negative (WT) hearts. These data are in apparent contrast to previous reports which show that EPHX2 ablation

increases coronary flow (49, 50), while transgenic EPHX2 overexpression reduces coronary flow (51); however, there are several substantive differences between those prior experiments and the current work. For example, previous data examined reactive hyperemia, which is the vascular response to brief (seconds) treatments of ischemia, while our experiment examined coronary flow after 20 min of global, no-flow ischemia. In our previous studies, the 20-min no-flow ischemia model has revealed differences in postischemic vasodilation in genetically modified mouse models or after pharmacological treatments (29). Although the postischemic increase in EETs may play a role in coronary vasodilation, this effect may be secondary to the more pronounced effects of nitric oxide and prostaglandins (52). Additionally, the retrograde perfusion method in the Langendorff system is significantly faster than normal coronary blood flow, which might attenuate any paracrine effects of EETs or obscure minor differences in coronary flow. While disruption of EPHX2 did not alter coronary flow in our experiments, it should be noted that EPHX2 may play a significant role in the development of cardiovascular disease or an acute response to myocardial infarction *in vivo*. Indeed, EPHX2 inhibition has been shown to reduce atherosclerosis in mice (15) and EPHX2 polymorphisms are associated with cardiovascular disease in humans (27). During a myocardial infarction, EPHX2 inhibition could elevate local EET levels in the coronary arteries which could subsequently promote thrombus disruption and/or vasodilation (1). Both effects would serve to promote rapid reperfusion of occluded arteries and improve postischemic outcomes.

In summary, our data from mice with cell-specific genetic disruption of *Ephx2* reveal that cardiac EPHX2 is primarily responsible for the majority of EPHX2-mediated EET hydrolysis in the heart and for regulating the recovery of function after I/R. Expression of EPHX2 in endothelial cells had little or no impact on vascular function or cardiac recovery after ischemia *ex vivo*. It is possible, however, that endothelial EPHX2 serves an important role in the progression of atherosclerosis and/or in acute vascular events during myocardial infarction. Our data suggest that the improved signaling and cardiac recovery after I/R observed following EPHX2 pharmacological inhibition is likely due to the suppression of EPHX2-mediated EET hydrolysis within cardiomyocytes.

Experimental procedures

Animals

C57BL/6 mice with an allele for conditional disruption of the *Ephx2* gene (*Ephx2*$^{tm1.1Arte}$) were generated by Artemis Pharmaceuticals. The recombinant *Ephx2* locus contains *LoxP* sites flanking the fourth and fifth exons (Fig. 1). Mice homozygous for the floxed allele without *Cre* expression were used as controls (*Ephx2*$^{fx/fx}$). Mice with endothelial-specific (*Ephx2*$^{fx/fx}$*/Tek-cre)* or cardiomyocyte-specific (*Ephx2*$^{fx/fx}$*/Myh6-cre)* disruption of *Ephx2* were bred by crossing *Ephx2*$^{fx/fx}$ mice with transgenic mice in which the *Cre* recombinase transgene was driven by either the *Tek (B6.Cg-Tg(Tek-Cre) 12Flv/J)* or *Myh6* (B6.FVB-Tg(Myh6-cre)2182Mds/J) promoter, respectively (Jackson Laboratory). Mice with conventional (global) disruption of *Ephx2* (global *Ephx2*$^{-/-}$) have been previously described (28). Approximately, equal numbers of male and female mice, aged 10 to 16 weeks, were used in each study. Mice were maintained in cages with a 12:12 h light-dark cycle and free access to standard chow (NIH31, Envigo) and water. All procedures were in accordance with the *NIH Guide for the Care and Use of Laboratory Animals* and were approved by the NIEHS Animal Care and Use Committee.

Immunohistochemistry

Tissues from mice were fixed in 10% neutral buffered formalin and embedded in paraffin. Sections (5 μm) were stained with anti-EPHX2 Ab (sc-22334, 1:100) from Santa Cruz Biotechnology and detected using biotinylated donkey-anti-goat secondary antibody (1:500) and diaminobenzidine detection as previously described (48).

Langendorff isolated-perfused hearts

Mice were anesthetized with pentobarbital, hearts were removed, cannulated by the aorta, and perfused in retrograde fashion in the Langendorff mode as previously described (3, 6, 29). Hearts were perfused with modified Krebs–Henseleit buffer, containing 120 mM NaCl, 25 mM $NaHCO_3$, 4.7 mM KCl, 1.2 mM KH_2PO_4, 1.20 mM $MgSO_4$, 11 mM glucose, and 1.8 mM $CaCl_2$, that was aerated with 95% air and 5% CO_2. Water-filled balloon pressure transducers were inserted into the left ventricle to monitor cardiac function. Forty minutes after cannulation, hearts were subjected to 20 min of global, no-flow ischemia, followed by up to 40 min of reperfusion. LVDP measured at the end of reperfusion was expressed as a percentage of pre-ischemic LVDP. RPP was calculated as LVDP × heart rate. In some experiments, 1 μM EEZE or vehicle (0.1% ethanol) were added to the perfusate starting 10 min prior to ischemia and throughout reperfusion. For signaling experiments, heart ventricles were cut from the cannula after 10 min of reperfusion. In separate experiments to collect heart perfusates for LC-MS/MS analysis, hearts were cannulated and perfused as above but without balloon insertion. All of the heart perfusate produced during the last 20 min of equilibration (baseline) and during the first 20 min of reperfusion were pooled and collected into 50 ml conical tubes with 5 μl of 10 mM *trans*-4-[4-(3-adamantan-1-yl-ureido)-cyclohexyloxy]-benzoic acid (kindly provided by Bruce Hammock, UC Davis). Perfusates were collected into tubes sitting in dry ice and stored at −80 °C prior to extraction and analysis.

mRNA analysis by quantitative RT-PCR

mRNA was isolated from heart tissues using RNeasy Mini Kits from Qiagen. mRNA was converted to complementary DNA using High-Capacity cDNA Reverse Transcription Kit from Life Technologies. *Ephx2* (#Mm00514706_m1) and *Gapdh* (Mm99999915_g1) were detected using TaqMan probes according to manufacturer's instructions. *Ephx2* expression was calculated relative to *Gapdh* using the $2^{-\Delta\Delta CT}$ method.

Protein immunoblotting

Hundred milligrams of heart tissue were added to 400 μl ice cold lysis buffer [1% Triton X-100, 0.25% deoxycholate,150 mM NaCl, 50 mM Tris (pH 7.4), plus EDTA/protease inhibitor cocktail (Roche)] and homogenized using a Tissuelyzer II with a single stainless-steel bead at 4 °C for 10 min at 30 Hz. The homogenate was centrifuged at 10,000*g* for 10 min. Supernatant was collected, and protein concentrations were determined by BCA Assay (Biorad). Twenty micrograms of protein was separated by 10% SDS-PAGE and transferred to nitrocellulose. Membranes were blocked with PBS containing 0.1% Tween 20 and 5% nonfat milk. Membranes were probed with antibodies to EPHX2 (sc-25797, 1:1000) and ERK1 (sc-93, 1:2000) from Santa Cruz Biotechnology, β-actin (AC-74, 1:5000) and pERK1/2 (M8159, 1:1000) from Sigma, and phospho-S21/9-GSK3β (9331) and GSK3β (9315) (1:1000 each) from Cell Signaling. Primary antibodies were detected using horseradish peroxidase-conjugated secondary antibodies from Calbiochem (#401215 and #401315, 1:5000 dilution) and enhanced chemiluminescence (Amersham). Densitometry was obtained and quantified on an Amersham Typhoon using ImageQuantTL v8.1.0 software (https://us.vwr.com/store/product/25990402/imagequant-tl-8-1-cytiva).

EET hydrolysis assay

Five hundred micrograms of heart lysate (lysed as above but in ice-cold PBS) were mixed with ice-cold solutions containing 50 ng of 14,15-EET, 11,12-EET, 12,13-EpOME, 19,20-EpDPE, or 17,18-EpETE (Cayman Chemical) in a total of 100 μl PBS containing 0.1% BSA. Samples were incubated at 37 °C for 10 min before reactions were stopped by the addition of 0.9 ml ethyl acetate. Ten microliters of internal standard [30 ng each of PGE_2-d9, 11,12-EET-d11, and 11,12-DHET-d11 (Cayman)] was added to each sample. Samples were mixed, centrifuged at 1000*g*, and ethyl acetate was removed to tubes containing 6 μl of 30% glycerol in methanol. Samples were dried under vacuum centrifugation, covered with argon gas, and stored at −80 °C. Rates of hydrolysis were determined by the formation of corresponding diols (14,15-DHET, 11,12-DHET, 12,13-DiHOME, 19,20-DiHDPE, or 17,18-DiHETE).

Cardiac perfusates

Samples were spiked with internal standards, mixed with 0.05 volume of 1% acetic acid in 50% methanol, and extracted by serial passage through HyperSep Retain C18 3 ml columns (Thermo Fisher Scientific). Columns were washed twice with 3 ml 0.05% acetic acid in 2.5% methanol. Analytes were eluted with 1 ml of methanol into glass tubes containing 6 μl of 30% glycerol in methanol. Samples were dried and stored at −80 °C as described above.

Liquid chromatography tandem mass spectroscopy

Samples were reconstituted in 50 μl of 30% ethanol. Liquid chromatography was performed with an Agilent 1200 Series capillary HPLC (Agilent Technologies). Separations were achieved using a Halo C18 column (2.7 μm, 100 × 2.1 mm; MAC-MOD Analytical) held at 50 °C. Mobile phase A (85:15:0.1 water:acetonitrile:acetic acid) and Mobile phase B (70:30:0.1 acetonitrile:methanol:acetic acid) were freshly prepared. Samples were injected at a flow rate of 400 μl/min with gradient elution. Mobile phase flow rates and percentages were varied as follows: the gradient ramped from 20% B at 0 min to 40% B at 5 min. Flow ramped from 40% B at 5 min to 55% B at 7 min and 64% B at 13 min. At 13 min, the column was flushed for 6 min with 100% B at a flow rate of 550 μl/min. Samples were reconstituted in 50 μl of 30% ethanol and triplicate samples were injected in a volume of 10 μl. Analytes were detected on an MDS Sciex API 3000 equipped with a TurboIonSpray source (Applied Biosystems) heated to 425 °C at a flow rate of 6 l/min. Detection was performed using negative ion electrospray ionization tandem mass spectrometry with multiple reaction monitoring as previously described (29). Oxylipin quantification was calculated using Analyst 1.5.1 software (AB Sciex; https://sciex.com/products/software/analyst-software). Relative response ratios of analytes to corresponding internal standards were compared to a standard curve of response ratios for each analyte. Lipid standards were purchased from Cayman Chemical, stored in 100% ethanol under argon, and used within 1 year.

Statistical analyses

Analysis of significance among the four genotypes was determined by one-way ANOVA followed by *post hoc* t-tests using GraphPad Prism (https://www.graphpad.com/features) and Microsoft Excel (https://www.microsoft.com/en-us/microsoft-365/excel) software. For cardiac perfusates, in addition to these comparisons, we conducted paired Student's t-tests to assess changes between baseline and postischemic analyte levels. Coronary flow rates were compared using repeated measure ANOVA. Mendelian analysis was performed using a Chi squared test of proportions. *p*-values less than 0.05 were considered significant.

Data availability

All data are contained within the article. The data that support the findings of this study are available from the corresponding author, D. C. Z. upon reasonable request.

Supporting information—This article contains supporting information.

Author contributions—M. L. E. and D. C. Z. formal analysis; M. L. E., A. G., J. A. B., J. P. G., F. B. L., and L. M. D. investigation; M. L. E. writing-original draft; M. L. E. and D. C. Z. writing-review and editing; M. L. E., I. F., and D. C. Z. visualization; M. L. E. and F. B. L. methodology; D. C. Z. supervision; M. L. E., A. G., and D. C. Z. conceptualization; M. L. E. data curation; D. C. Z. project administration; D. C. Z. and I. F. funding acquisition.

Funding and additional information—This work was supported, in part, by the Division of Intramural Research, National Institute of Environmental Health Sciences, NIH (Z01 ES025034) to D. C. Z.

and by the Deutsche Forschungsgemeinschaft SFB 834/3 project B13 grant to I. F. The content is solely the responsibility of the authors and does not necessarily represent the official views of the National Institutes of Health.

Conflicts of interest—The authors declare that they have no conflicts of interest with the contents of this article.

Abbreviations—The abbreviations used are: DHA, docosahexaenoic acid; DHET, dihydroxyeicosatrienoic acid; EET, epoxyeicosatrienoic acid; EEZE, 14,15-epoxyeicosa-5(Z)-enoic acid; EPA, eicosapentaenoic acid; EpDPE, epoxydocosapentaenoic acid; EpETE, epoxyeicosatetraenoic acid; EpFA, epoxy-fatty acid; EPHX, epoxide hydrolase; EPHX1, microsomal epoxide hydrolase; EPHX2, soluble epoxide hydrolase; I/R, ischemia/reperfusion; K_{ATP}, ATP-sensitive K+ channels; LA, linoleic acid; LVDP, left ventricular developed pressure; mPTP, mitochondrial permeability transition pore; RPP, rate pressure product.

References

1. Spector, A. A., and Norris, A. W. (2007) Action of epoxyeicosatrienoic acids on cellular function. *Am. J. Physiol. Cell Physiol.* **292**, C996–C1012
2. Westphal, C., Konkel, A., and Schunck, W. H. (2011) CYP-eicosanoids–a new link between omega-3 fatty acids and cardiac disease? *Prostaglandins Other Lipid Mediat.* **96**, 99–108
3. Edin, M. L., Hamedani, B. G., Gruzdev, A., Graves, J. P., Lih, F. B., Arbes, S. J., 3rd, *et al.* (2018) Epoxide hydrolase 1 (EPHX1) hydrolyzes epoxyeicosanoids and impairs cardiac recovery after ischemia. *J. Biol. Chem.* **293**, 3281–3292
4. Morisseau, C., and Hammock, B. D. (2013) Impact of soluble epoxide hydrolase and epoxyeicosanoids on human health. *Annu. Rev. Pharmacol. Toxicol.* **53**, 37–58
5. Chaudhary, K. R., Abukhashim, M., Hwang, S. H., Hammock, B. D., and Seubert, J. M. (2010) Inhibition of soluble epoxide hydrolase by trans-4-[4-(3-adamantan-1-yl-ureido)-cyclohexyloxy]-benzoic acid is protective against ischemia-reperfusion injury. *J. Cardiovasc. Pharmacol.* **55**, 67–73
6. Seubert, J. M., Sinal, C. J., Graves, J., DeGraff, L. M., Bradbury, J. A., Lee, C. R., *et al.* (2006) Role of soluble epoxide hydrolase in postischemic recovery of heart contractile function. *Circ. Res.* **99**, 442–450
7. Litvinukova, M., Talavera-Lopez, C., Maatz, H., Reichart, D., Worth, C. L., Lindberg, E. L., *et al.* (2020) Cells of the adult human heart. *Nature* **588**, 466–472
8. Banerjee, I., Fuseler, J. W., Price, R. L., Borg, T. K., and Baudino, T. A. (2007) Determination of cell types and numbers during cardiac development in the neonatal and adult rat and mouse. *Am. J. Physiol. Heart Circ. Physiol.* **293**, H1883–H1891
9. Larsen, B. T., Miura, H., Hatoum, O. A., Campbell, W. B., Hammock, B. D., Zeldin, D. C., *et al.* (2006) Epoxyeicosatrienoic and dihydroxyeicosatrienoic acids dilate human coronary arterioles via BK(Ca) channels: implications for soluble epoxide hydrolase inhibition. *Am. J. Physiol. Heart Circ. Physiol.* **290**, H491–H499
10. Enayetallah, A. E., French, R. A., Thibodeau, M. S., and Grant, D. F. (2004) Distribution of soluble epoxide hydrolase and of cytochrome P450 2C8, 2C9, and 2J2 in human tissues. *J. Histochem. Cytochem.* **52**, 447–454
11. Yu, Z., Davis, B. B., Morisseau, C., Hammock, B. D., Olson, J. L., Kroetz, D. L., *et al.* (2004) Vascular localization of soluble epoxide hydrolase in the human kidney. *Am. J. Physiol. Renal Physiol.* **286**, F720–F726
12. Enayetallah, A. E., French, R. A., Barber, M., and Grant, D. F. (2006) Cell-specific subcellular localization of soluble epoxide hydrolase in human tissues. *J. Histochem. Cytochem.* **54**, 329–335
13. Davis, B. B., Thompson, D. A., Howard, L. L., Morisseau, C., Hammock, B. D., and Weiss, R. H. (2002) Inhibitors of soluble epoxide hydrolase attenuate vascular smooth muscle cell proliferation. *Proc. Natl. Acad. Sci. U. S. A.* **99**, 2222–2227
14. Deng, Y., Edin, M. L., Theken, K. N., Schuck, R. N., Flake, G. P., Kannon, M. A., *et al.* (2011) Endothelial CYP epoxygenase overexpression and soluble epoxide hydrolase disruption attenuate acute vascular inflammatory responses in mice. *FASEB J.* **25**, 703–713
15. Ulu, A., Davis, B. B., Tsai, H. J., Kim, I. H., Morisseau, C., Inceoglu, B., *et al.* (2008) Soluble epoxide hydrolase inhibitors reduce the development of atherosclerosis in apolipoprotein e-knockout mouse model. *J. Cardiovasc. Pharmacol.* **52**, 314–323
16. Node, K., Ruan, X. L., Dai, J., Yang, S. X., Graham, L., Zeldin, D. C., *et al.* (2001) Activation of galpha s mediates induction of tissue-type plasminogen activator gene transcription by epoxyeicosatrienoic acids. *J. Biol. Chem.* **276**, 15983–15989
17. Campbell, W. B., Gebremedhin, D., Pratt, P. F., and Harder, D. R. (1996) Identification of epoxyeicosatrienoic acids as endothelium-derived hyperpolarizing factors. *Circ. Res.* **78**, 415–423
18. Seubert, J. M., Zeldin, D. C., Nithipatikom, K., and Gross, G. J. (2007) Role of epoxyeicosatrienoic acids in protecting the myocardium following ischemia/reperfusion injury. *Prostaglandins Other Lipid Mediat.* **82**, 50–59
19. Batchu, S. N., Chaudhary, K. R., El-Sikhry, H., Yang, W., Light, P. E., Oudit, G. Y., *et al.* (2012) Role of PI3Kalpha and sarcolemmal ATP-sensitive potassium channels in epoxyeicosatrienoic acid mediated cardioprotection. *J. Mol. Cell. Cardiol.* **53**, 43–52
20. Murphy, E., and Steenbergen, C. (2005) Inhibition of GSK-3beta as a target for cardioprotection: the importance of timing, location, duration and degree of inhibition. *Expert Opin. Ther. Targets* **9**, 447–456
21. Lu, T., Hoshi, T., Weintraub, N. L., Spector, A. A., and Lee, H. C. (2001) Activation of ATP-sensitive K(+) channels by epoxyeicosatrienoic acids in rat cardiac ventricular myocytes. *J. Physiol.* **537**, 811–827
22. Samokhvalov, V., Jamieson, K. L., Darwesh, A. M., Keshavarz-Bahaghighat, H., Lee, T. Y. T., Edin, M., *et al.* (2018) Deficiency of soluble epoxide hydrolase protects cardiac function impaired by LPS-induced acute inflammation. *Front. Pharmacol.* **9**, 1572
23. Zhao, W. Y., Zhang, X. Y., Zhou, M. R., Tian, X. G., Lv, X., Zhang, H. L., *et al.* (2021) Natural soluble epoxide hydrolase inhibitors from Alisma orientale and their potential mechanism with soluble epoxide hydrolase. *Int. J. Biol. Macromol.* **183**, 811–817
24. Monti, J., Fischer, J., Paskas, S., Heinig, M., Schulz, H., Gosele, C., *et al.* (2008) Soluble epoxide hydrolase is a susceptibility factor for heart failure in a rat model of human disease. *Nat. Genet.* **40**, 529–537
25. Althurwi, H. N., Tse, M. M., Abdelhamid, G., Zordoky, B. N., Hammock, B. D., and El-Kadi, A. O. (2013) Soluble epoxide hydrolase inhibitor, TUPS, protects against isoprenaline-induced cardiac hypertrophy. *Br. J. Pharmacol.* **168**, 1794–1807
26. Oni-Orisan, A., Cresci, S., Jones, P. G., Theken, K. N., Spertus, J. A., and Lee, C. R. (2018) Association between the EPHX2 p.Lys55Arg polymorphism and prognosis following an acute coronary syndrome. *Prostaglandins Other Lipid Mediat.* **138**, 15–22
27. Lee, C. R., North, K. E., Bray, M. S., Fornage, M., Seubert, J. M., Newman, J. W., *et al.* (2006) Genetic variation in soluble epoxide hydrolase (EPHX2) and risk of coronary heart disease: the Atherosclerosis Risk in Communities (ARIC) study. *Hum. Mol. Genet.* **15**, 1640–1649
28. Sinal, C. J., Miyata, M., Tohkin, M., Nagata, K., Bend, J. R., and Gonzalez, F. J. (2000) Targeted disruption of soluble epoxide hydrolase reveals a role in blood pressure regulation. *J. Biol. Chem.* **275**, 40504–40510
29. Edin, M. L., Wang, Z., Bradbury, J. A., Graves, J. P., Lih, F. B., DeGraff, L. M., *et al.* (2011) Endothelial expression of human cytochrome P450 epoxygenase CYP2C8 increases susceptibility to ischemia-reperfusion injury in isolated mouse heart. *FASEB J.* **25**, 3436–3447
30. Seubert, J., Yang, B., Bradbury, J. A., Graves, J., Degraff, L. M., Gabel, S., *et al.* (2004) Enhanced postischemic functional recovery in CYP2J2 transgenic hearts involves mitochondrial ATP-sensitive K+ channels and p42/p44 MAPK pathway. *Circ. Res.* **95**, 506–514
31. Gauthier, K. M., Deeter, C., Krishna, U. M., Reddy, Y. K., Bondlela, M., Falck, J. R., *et al.* (2002) 14,15-Epoxyeicosa-5(Z)-enoic acid: a selective epoxyeicosatrienoic acid antagonist that inhibits endothelium-dependent hyperpolarization and relaxation in coronary arteries. *Circ. Res.* **90**, 1028–1036

32. Birkenmeier, K., Staudt, A., Schunck, W. H., Janke, I., Labitzke, C., Prange, T., *et al.* (2007) COX-2-dependent and potentially cardioprotective effects of negative inotropic substances released after ischemia. *Am. J. Physiol. Heart Circ. Physiol.* **293**, H2148–H2154
33. Lu, M. J., Chen, Y. S., Huang, H. S., and Ma, M. C. (2014) Hypoxic preconditioning protects rat hearts against ischemia-reperfusion injury via the arachidonate12-lipoxygenase/transient receptor potential vanilloid 1 pathway. *Basic Res. Cardiol.* **109**, 414
34. Kerkela, R., Boucher, M., Zaka, R., Gao, E., Harris, D., Piuhola, J., *et al.* (2011) Cytosolic phospholipase A(2)alpha protects against ischemia/reperfusion injury in the heart. *Clin. Transl Sci.* **4**, 236–242
35. Mancuso, D. J., Abendschein, D. R., Jenkins, C. M., Han, X., Saffitz, J. E., Schuessler, R. B., *et al.* (2003) Cardiac ischemia activates calcium-independent phospholipase A2beta, precipitating ventricular tachyarrhythmias in transgenic mice: rescue of the lethal electrophysiologic phenotype by mechanism-based inhibition. *J. Biol. Chem.* **278**, 22231–22236
36. Moon, S. H., Liu, X., Cedars, A. M., Yang, K., Kiebish, M. A., Joseph, S. M., *et al.* (2018) Heart failure-induced activation of phospholipase iPLA(2)gamma generates hydroxyeicosatetraenoic acids opening the mitochondrial permeability transition pore. *J. Biol. Chem.* **293**, 115–129
37. Karara, A., Wei, S., Spady, D., Swift, L., Capdevila, J. H., and Falck, J. R. (1992) Arachidonic acid epoxygenase: structural characterization and quantification of epoxyeicosatrienoates in plasma. *Biochem. Biophys. Res. Commun.* **182**, 1320–1325
38. Spector, A. A. (2009) Arachidonic acid cytochrome P450 epoxygenase pathway. *J. Lipid Res.* **50 Suppl**(Suppl), S52–S56
39. Edin, M. L., and Zeldin, D. C. (2021) Regulation of cardiovascular biology by microsomal epoxide hydrolase. *Toxicol. Res.* **37**, 285–292
40. Fang, X., Weintraub, N. L., McCaw, R. B., Hu, S., Harmon, S. D., Rice, J. B., *et al.* (2004) Effect of soluble epoxide hydrolase inhibition on epoxyeicosatrienoic acid metabolism in human blood vessels. *Am. J. Physiol. Heart Circ. Physiol.* **287**, H2412–H2420
41. Klett, E. L., Chen, S., Edin, M. L., Li, L. O., Ilkayeva, O., Zeldin, D. C., *et al.* (2013) Diminished acyl-CoA synthetase isoform 4 activity in INS 832/13 cells reduces cellular epoxyeicosatrienoic acid levels and results in impaired glucose-stimulated insulin secretion. *J. Biol. Chem.* **288**, 21618–21629
42. Fang, X., Weintraub, N. L., Oltman, C. L., Stoll, L. L., Kaduce, T. L., Harmon, S., *et al.* (2002) Human coronary endothelial cells convert 14, 15-EET to a biologically active chain-shortened epoxide. *Am. J. Physiol. Heart Circ. Physiol.* **283**, H2306–H2314
43. Greene, J. F., Newman, J. W., Williamson, K. C., and Hammock, B. D. (2000) Toxicity of epoxy fatty acids and related compounds to cells expressing human soluble epoxide hydrolase. *Chem. Res. Toxicol.* **13**, 217–226
44. Fukushima, A., Hayakawa, M., Sugiyama, S., Ajioka, M., Ito, T., Satake, T., *et al.* (1988) Cardiovascular effects of leukotoxin (9, 10-epoxy-12-octadecenoate) and free fatty acids in dogs. *Cardiovasc. Res.* **22**, 213–218
45. Konkel, A., and Schunck, W. H. (2011) Role of cytochrome P450 enzymes in the bioactivation of polyunsaturated fatty acids. *Biochim. Biophys. Acta* **1814**, 210–222
46. Hercule, H. C., Salanova, B., Essin, K., Honeck, H., Falck, J. R., Sausbier, M., *et al.* (2007) The vasodilator 17,18-epoxyeicosatetraenoic acid targets the pore-forming BK alpha channel subunit in rodents. *Exp. Physiol.* **92**, 1067–1076
47. Imig, J. D., Cervenka, L., and Neckar, J. (2022) Epoxylipids and soluble epoxide hydrolase in heart diseases. *Biochem. Pharmacol.* **195**, 114866
48. Lee, C. R., Imig, J. D., Edin, M. L., Foley, J., DeGraff, L. M., Bradbury, J. A., *et al.* (2010) Endothelial expression of human cytochrome P450 epoxygenases lowers blood pressure and attenuates hypertension-induced renal injury in mice. *FASEB J.* **24**, 3770–3781
49. Hanif, A., Edin, M. L., Zeldin, D. C., Morisseau, C., Falck, J. R., Ledent, C., *et al.* (2017) Reduced coronary reactive hyperemia in mice was reversed by the soluble epoxide hydrolase inhibitor (t-AUCB): role of adenosine A2A receptor and plasma oxylipins. *Prostaglandins Other Lipid Mediat.* **131**, 83–95
50. Hanif, A., Edin, M. L., Zeldin, D. C., Morisseau, C., and Nayeem, M. A. (2016) Deletion of soluble epoxide hydrolase enhances coronary reactive hyperemia in isolated mouse heart: role of oxylipins and PPARgamma. *Am. J. Physiol. Regul. Integr. Comp. Physiol.* **311**, R676–R688
51. Hanif, A., Edin, M. L., Zeldin, D. C., Morisseau, C., Falck, J. R., and Nayeem, M. A. (2017) Vascular endothelial over-expression of human soluble epoxide hydrolase (Tie2-sEH Tr) attenuates coronary reactive hyperemia in mice: role of oxylipins and omega-hydroxylases. *PLoS One* **12**, e0169584
52. Ellinsworth, D. C., Sandow, S. L., Shukla, N., Liu, Y., Jeremy, J. Y., and Gutterman, D. D. (2016) Endothelium-derived hyperpolarization and coronary vasodilation: diverse and integrated roles of epoxyeicosatrienoic acids, hydrogen peroxide, and gap junctions. *Microcirculation* **23**, 15–32